Developmental Cell, Vol. 3, 1–20, June, 2002, Copyright ©2002 by Cell Press

Regulated SUMOylation and Ubiquitination of DdMEK1 Is Required for Proper Chemotaxis

Alex Sobko, Hui Ma,[2] and Richard A. Firtel[1]
Section of Cell and Developmental Biology
Division of Biology
University of California, San Diego
9500 Gilman Drive
La Jolla, California 92093

Summary

MEK1, which is required for aggregation and chemotaxis in *Dictyostelium*, is rapidly and transiently SUMOylated in response to chemoattractant stimulation. SUMOylation is required for MEK1's function and its translocation from the nucleus to the cytosol and cortex, including the leading edge of chemotaxing cells. MEK1 in which the site of SUMOylation is mutated is retained in the nucleus and does not complement the *mek1* null phenotype. Constitutively active MEK1 is cytosolic and is constitutively SUMOylated, whereas the corresponding nonactivatable MEK1 is not SUMOylated and nuclear. MEK1 is also ubiquitinated in response to signaling. A MEK1-interacting, ubiquitin E3 ligase RING domain-containing protein controls nuclear localization and MEK1 ubiquitination. These studies provide a pathway regulating the localization and function of MEK1.

Introduction

Chemotaxis, a form of directed cell movement, is a basic property exhibited by many motile cells and can be stimulated by chemoattractants that bind to and activate pathways downstream from G protein-coupled receptors and receptor protein tyrosine kinases. Recent studies have demonstrated that signaling pathways that control chemotaxis are highly conserved in diverse cell types, including leukocytes, fibroblasts, and *Dictyostelium* amoebae (Chung et al., 2001; Parent and Devreotes, 1999; Rickert et al., 2000).

In *Dictyostelium*, a MAP kinase cascade was previously identified that is required for chemotaxis toward cAMP, the chemoattractant that mediates the aggregation response, leading to the formation of a multicellular organism (Ma et al., 1997). Null mutants of the *Dictyostelium* MAP kinase kinase MEK1 are unable to properly chemotax and form extremely small aggregates, presumably through cell-cell adhesion contacts rather than chemoattractant-mediated aggregation. A constitutively active MEK1 (MEK1^{S444E,T448E}) in which the serine and threonine phosphorylation sites in the activation loop are mutated to glutamate complements the *mek1* null cell chemotaxis defect, but this strain is unable to undergo proper morphogenesis upon reaching the mound stage. MEK1^{S444A,T448A}, which cannot be activated, does not complement the null mutation and functions as a dominant interfering (negative) protein when expressed in wild-type cells. Studies examining the phenotypes of a temperature-sensitive allele of MEK1 suggest that MEK1 is required at the time of chemoattractant-mediated stimulation to control chemotaxis (Ma et al., 1997). Recent studies indicate that embryonic fibroblasts from *mek1*$^{-/-}$ or *mekk1*$^{-/-}$ mice have defects in cell migration, suggesting that this function could be evolutionarily conserved between *Dictyostelium* and vertebrate MAP kinase pathways (Giroux et al., 1999; Yujiri et al., 2000).

SUMO is a ubiquitin-related protein that, like ubiquitin, is covalently attached to a lysine residue on the substrate protein via a pathway similar to ubiquitination (Hochstrasser, 2001; Melchior, 2000; Muller et al., 2001; Bernier-Villamor et al., 2002). SUMOylation has been implicated in the control of subcellular protein localization and/or proteasomal degradation of several substrate proteins (reviewed in Muller et al., 2001). For example, SUMOylation can oppose ubiquitination and proteasomal degradation by competitive attachment to the same lysine residues within substrate proteins, as is the case for IκB (Desterro et al., 1998) and MDM2 (Buschmann et al., 2000).

In this manuscript, we demonstrate that *Dictyostelium* MEK1 is SUMOylated in response to chemoattractant stimulation and that this modification plays a central role in regulating MEK1's subcellular localization and function. MEK1 is also ubiquitinated and the level of polyubiquitinated MEK1 increases in response to chemoattractant stimulation, with kinetics that are delayed compared to those of SUMOylation. We identified the MEK1-interacting protein MIP1 and present genetic and biochemical evidence that MIP1 functions as a MEK1-specific E3 ubiquitin ligase and controls MEK1's nuclear localization. These results provide new insights into the mechanisms controlling chemotaxis and the differential role of the SUMOylation and ubiquitination pathways in controlling subcellular localization and the regulation of MAP kinase cascades.

Results

Dictyostelium MEK1 Is Transiently SUMOylated in Response to Chemoattractant Stimulation

We examined whether *Dictyostelium* MEK1 is transiently modified in response to chemoattractant stimulation by expressing FLAG- or myc-tagged versions of MEK1 in either *mek1* null (Ma et al., 1997) or wild-type cells (strain KAx-3). Expression of either tagged MEK1 complemented the *mek1* null phenotypes and produced indistinguishable results (Figures 1B and 1C; data for myc-tagged MEK1 is not shown). Upon stimulation of "aggregation-competent" *Dictyostelium* cells by the chemoattractant cAMP, there is a transient shift of the mobility of a portion of MEK1 from an apparent molecular weight of ~75 to ~90 kDa on SDS-PAGE gels (Figure 1A). The maximal shift occurs between 5 and 15 s (15 s time point is shown)

[1]Correspondence: rafirtel@ucsd.edu
[2]Present address: Salk Institute for Biological Sciences, 10010 North Torrey Pines Road, La Jolla, California 92037.

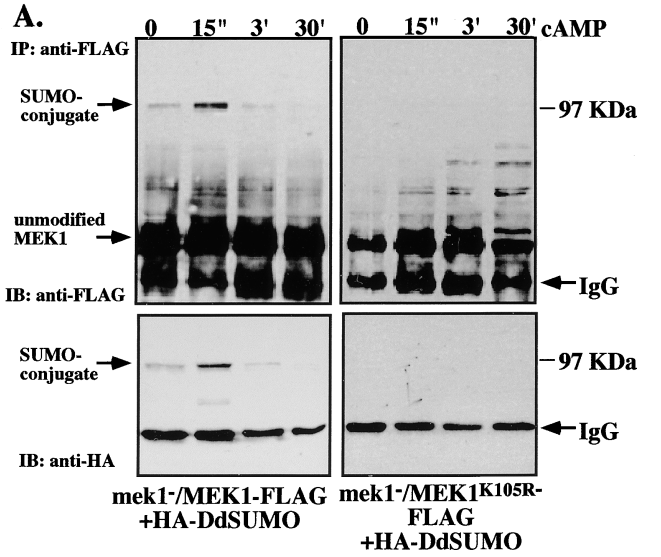

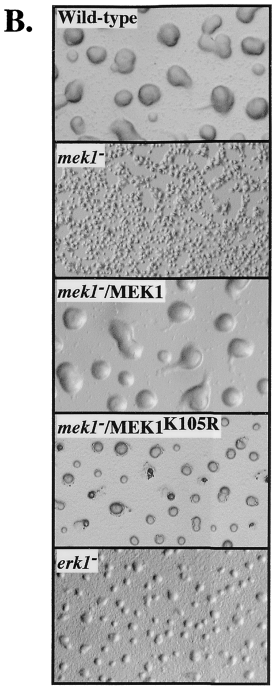

C.

Genotype (Strain)	Speed (μm/min)	Directional change (deg)	Roundness (%)	Directionality
Wild-type (KAx-3)	8.5±0.5	12.5±4.4	43.8±4.2	0.90±0.6
mek1-/MEK1 (ASF1)	8.1±0.4	12.4±0.8	41.3±4.8	0.89±0.05
mip1 null (HMF3)	5.7±0.3	41.1±4.5	51.9±0.7	0.59±0.06
mek1-/MEK1K105R (ASF2)	5.0±0.4	42.6±4.4	45.9±6.1	0.66±0.04
KAx-3 /MEK1K105R (ASF3)	5.9±0.7	37.9 ±8.1	40.2±10.0	0.69±0.03
mek1 null (HMF1)	3.2±0.3	67.0±5.2	76.8±7.5	0.19±0.01
erk1 null (HMF2)	4.2±3.1	51.0±5.1	74.8±7.6	0.10±0.03

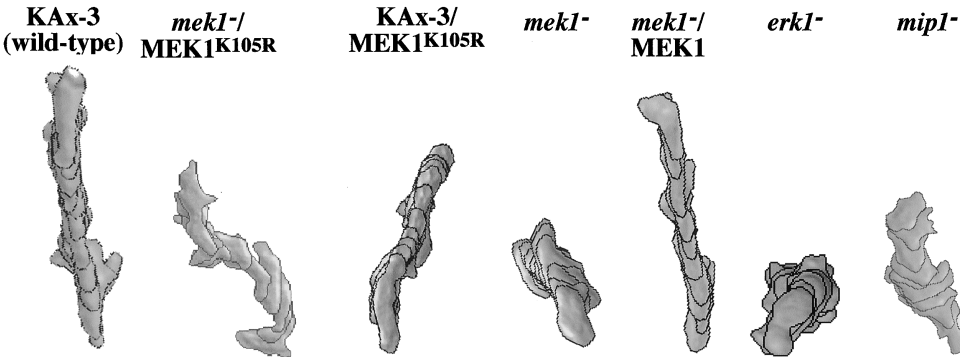

Figure 1. MEK1 SUMOylation and Its Role in Aggregation and Chemotaxis

(A) MEK1 is SUMOylated on K105. *mek1* null cells coexpressing HA-DdSUMO and either MEK1-FLAG (left panel) or MEK1^{K105R}-FLAG (right panel) were pulsed every 6 min with 30 nM cAMP for 5 hr, stimulated with 30 μM cAMP for the indicated time intervals, and lysed as described in Experimental Procedures. Immunoprecipitated MEK1 was subjected to immunoblot analysis with anti-FLAG and anti-HA antibodies.

(B) The morphology of *mek1*, *erk1*$^-$, and *mek1*$^-$ cells expressing either MEK1-FLAG or MEK1^{K105R}-FLAG at the aggregation stage of development.

(C) Chemotaxis of wild-type cells, *mek1* and *erk1* null cells, and *mek1* null or wild-type KAx-3 cells expressing MEK1^{K105R}. Time-lapse recording and quantitative analysis showing the chemotaxis defects of cells moving toward a pipette filled with 150 μM cAMP. Superimposed images show the cell shapes, direction, and length of the path during chemotaxis at 1 min intervals. When *mek1* null cells are pulsed for a longer time (see Experimental Procedures), the cells become more polarized but still exhibit significant chemotaxis defects (data not shown.) The strain names and genotypes are given in the table. All strains have been made in the KAx-3 wild-type background.

after stimulation and then decreases to background levels by 1–3 min. As shown in Figure 1, there is a very low basal level of the 90 kDa isoform of MEK1 in unstimulated cells, presumably due to the repetitive cycles of cAMP stimulation used to maximally express components of the signaling pathway to make cells responsive to cAMP ("aggregation-competent" cells).

The observation of a major molecular species shifted by ~15 kDa and the presence of putative SUMOylation consensus sites (I/LKXE; Sampson et al., 2001; Bernier-Villamor et al., 2002) in MEK1 (MEK1^{K70} and MEK1$^{K105)}$ suggested that MEK1 might be SUMOylated. We tested this hypothesis by coexpressing *Dictyostelium* MEK1-FLAG and HA-tagged *Dictyostelium* SUMO (GenBank accession number AF446008; see Experimental Procedures). The MEK1-FLAG was immunoprecipitated with an anti-FLAG antibody and the blot was probed with either an anti-FLAG or anti-HA antibody. An ~90 kDa band was detected by both the anti-FLAG and anti-HA antibodies (Figure 1A). This band had the same mobility as that identified with an anti-human SUMO antibody (data not shown; see below).

To examine whether K70 or K105 is the site of SUMOylation, we expressed in wild-type cells MEK1 in which these lysines were individually mutated to arginines, and chemoattractant-mediated SUMOylation was examined. MEK1^{K105R} was not SUMOylated (Figure 1A), whereas MEK1^{K70R} was SUMOylated (data not shown), indicating that K105 is the site of MEK1 SUMOylation. To examine the biological consequences of MEK1 SUMOylation, we expressed MEK1^{K105R} in *mek1* null and wild-type cells (strain KAx-3). Time-lapse video microscopy and imaging of the development of *mek1* null cells expressing FLAG- or myc-tagged MEK1^{K105R} revealed that MEK1^{K105R} was unable to properly complement the *mek1* null phenotype; this strain produced significantly smaller aggregates than wild-type cells, although the size of the aggregates was larger than those of *mek1* null cells (Figure 1B; data for time-lapse microscopy not shown). Many *mek1*$^-$/MEK1^{K105R} cells fail to enter the aggregates, apparently due to chemotaxis defects (see below). Wild-type cells expressing MEK1^{K105R} also produced small aggregates, indicating that SUMOylation-deficient MEK1^{K105R} functions as a dominant-negative protein.

To confirm that *mek1*$^-$/MEK1^{K105R} cells are defective in chemotaxis, we examined the ability of *mek1* null cells, wild-type cells, *mek1*$^-$/MEK1^{K105R} cells, and wild-type cells expressing MEK1^{K105R} (KAx-3/MEK1^{K105R}) to chemotax toward a micropipette containing cAMP (Chung and Firtel, 1999; Meili et al., 1999). Whereas wild-type cells rapidly chemotax toward a micropipette emitting cAMP and produce few lateral pseudopodia (Figure 1C), *mek1* null cells are unable to do so, as previously demonstrated using a less quantitative assay (Ma et al., 1997). *mek1* null cells are significantly less polarized than wild-type cells, move considerably more slowly, and exhibit multiple directional changes, probably due to the extension of pseudopodia from the sides of the cell, as determined by DIAS computer analysis (Soll and Wessels, 1998). *mek1*$^-$/MEK1^{K105R} cells showed a similar chemotaxis defect, although not as extreme as that of *mek1* null cells (Figure 1C), suggesting that SUMOylation is required for proper MEK1 function. Expression of MEK1^{K105R} in wild-type cells resulted in chemotaxis defects that were similar to those of *mek1*$^-$/MEK1^{K105R} cells (Figure 1C), consistent with the aggregation defect exhibited by this strain.

MEK1 Translocates to the Cell Cortex in Response to Chemoattractant Stimulation and Is Found at the Leading Edge of Chemotaxing Cells

Since GFP-tagged MEK1 (placed at either the N or C terminus) did not effectively complement the *mek1* null phenotype, we examined the subcellular localization of MEK1 using FLAG-tagged MEK1 expressed in *mek1* null or wild-type cells by indirect immunofluorescence using deconvolution microscopy and analyzed the data with SoftWorx software (Agard et al., 1989). In unstimulated, aggregation-competent cells or vegetatively growing cells, FLAG-tagged MEK1 was found predominantly in the nucleus (Figures 2A and 2B). Upon cAMP stimulation of aggregation-competent cells, a portion of MEK1 transiently translocated to the cytosol and cell cortex. The timing of this change in MEK1 subcellular localization was similar to that of MEK1 SUMOylation, with maximal cortical and cytoplasmic localization at 5 to 15 s after stimulation (Figures 2A, 2B, 2E, and 2F). Quantitative analysis of fluorescence intensities (Figure 2F) revealed a significant increase of MEK1 concentration in the cell cortex at 15 s after stimulation. There is a concomitant decrease in nuclear MEK1 (see below). By 3 min, the level of cortical localization was significantly reduced. In chemotaxing cells, FLAG-MEK1 is highly enriched at the leading edge, colocalizing with F-actin (Figure 2D).

Figure 2A shows that a fraction of HA-tagged SUMO colocalized with FLAG-tagged MEK1 in the areas of the cell cortex after chemoattractant stimulation. This result was further confirmed using the anti-SUMO antibody (data not shown). Both MEK1 and SUMO proteins displayed similar kinetics of cortical localization, consistent with cortically localized SUMO being, at least in part, conjugated to MEK1, although we cannot rule out the possibility that we are also visualizing SUMO conjugated to other proteins. To determine whether SUMOylation may be required for this change in MEK1 localization, we examined the subcellular localization of FLAG-MEK1^{K105R} expressed in either *mek1* null or wild-type cells. Quantitative analysis shows that, like wild-type FLAG-MEK1, FLAG-MEK1^{K105R} is predominantly nuclear in unstimulated cells; however, in contrast to wild-type MEK1, MEK1^{K105R} does not exhibit a significant increase of cortical localization in response to cAMP stimulation (Figures 2C and 2F). These results are consistent with SUMOylation being required for MEK1 translocation. The inability of MEK1^{K105R} to localize at the plasma membrane may be, at least in part, responsible for the *mek1*$^-$/MEK1^{K105R} cell chemotaxis and aggregation defects.

ERK1 Lies Downstream from MEK1 and Exhibits a Chemoattractant-Mediated Relocalization

Previous analysis suggested that ERK1 is involved in aggregation and/or morphogenesis (Gaskins et al., 1994). An *erk1* insertional mutant was obtained in a random mutagenesis screen for *Dictyostelium* developmental mutants (http://www-biology.ucsd.edu/others/dsmith/dictydb.html). Using this information, we made

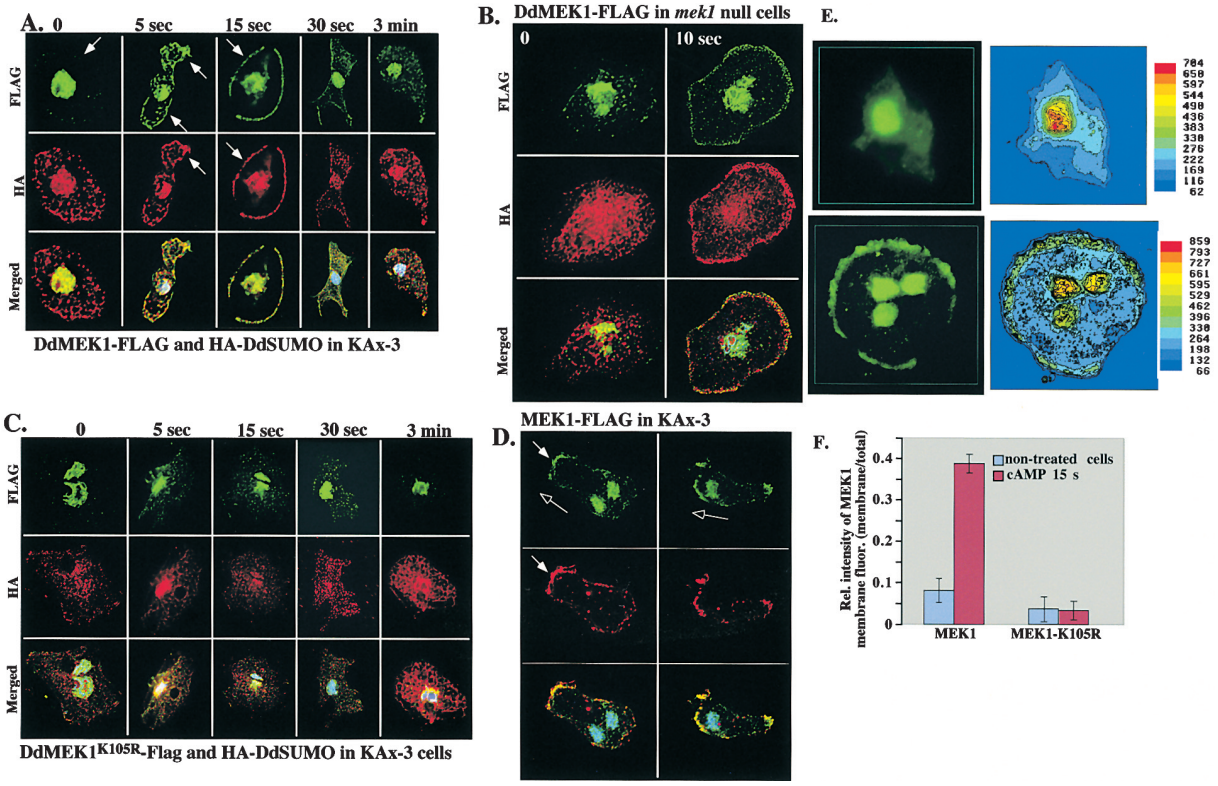

Figure 2. Immunofluorescence Analysis of the Localization of MEK1 and SUMO

(A) Translocation of MEK1-FLAG and HA-DdSUMO to the cell cortex in response to global cAMP stimulation in KAx-3 cells analyzed by indirect immunofluorescence and DeltaVision deconvolution microscopy. Arrows point to the cortically localized MEK1. Every image represents deconvolved integration of multiple optical sections through the given cell sample (see Experimental Procedures).

(B) MEK1 translocation to the plasma membrane 10 s after cAMP stimulation. The same pattern of MEK1 localization and translocation was observed in *mek1* null cells expressing MEK1. The lower panel includes nuclear (Hoechst) staining (blue).

(C) Retention of MEK1^{K105R} in the nucleus. In the wild-type KAx-3 cells and in *mek1* null cells (data not shown), SUMOylation-deficient mutant MEK1^{K105R} does not translocate to the cytosol and cell membrane in response to cAMP.

(D) Localization of MEK1 (green) and F-actin (red) in chemotaxing cells. The open arrow shows the direction of cell movement toward the center of the aggregation stream.

(E) Distribution of MEK1^{K105R} (upper panel) and wild-type MEK1 (lower panel) fluorescence (produced using SoftWorx) throughout representative cells at 15 s after stimulation. The color scale shows the range of fluorescence intensities in the cell.

(F) Comparison of relative intensities of MEK1 fluorescence in the cell cortex between the wild-type MEK1 and MEK1^{K105R} (n = 20; see Experimental Procedures for the details of the quantitative analysis).

a new *erk1* null strain. Figures 1B and 1C show that *erk1* null cells exhibited developmental and chemotaxis defects similar to those of *mek1* null cells (see below), suggesting that MEK1 and ERK1 are in the same regulatory cascade. This conclusion was supported by the observation that *erk1* null cells expressing constitutively active MEK1 (MEK1^{S444E,T448E}) exhibited the same phenotypes as *erk1* null cells (data not shown), consistent with an epistatic relationship. Further, ERK1 kinase is activated by chemoattractant stimulation in wild-type cells with maximal activity at the 15 s time point (Figure 3A). No cAMP-stimulated ERK1 activity was observed in *mek1* null cells. These findings are consistent with ERK1 lying downstream from MEK1. *erk1* null aggregates were slightly larger and the chemotaxis defects appeared to be less severe than in *mek1* null cells, suggesting that MEK1 may have functions in addition to the activation of ERK1.

We examined the subcellular localization of ERK1 in wild-type and *mek1* null cells, using a myc-tagged ERK1 construct that complements the *erk1* null cell phenotypes (data not shown). In contrast to MEK1, ERK1 was cytosolic rather than nuclear in unstimulated cells. Upon chemoattractant stimulation, ERK1 became partially localized to the cell's cortex, as does MEK1 (Figure 3B). This cortical localization of ERK1 overlaps that of F-actin. In chemotaxing cells, ERK1 is partially localized to the leading edge (Figure 3E). It is, however, absent in most distal parts of F-actin-enriched membrane protrusions. ERK1 did not become visibly cortically localized in *mek1* null cells (Figure 3C), indicating a requirement of MEK1 function for ERK1 cortical localization. These results are consistent with ERK1 cortical localization being associated with its activation by MEK1. (Colocalization of ERK1 and MEK1 and ERK1 activity in the strains expressing MEK1 mutants could not be examined, as we could not obtain stable transformants overexpressing both tagged proteins.)

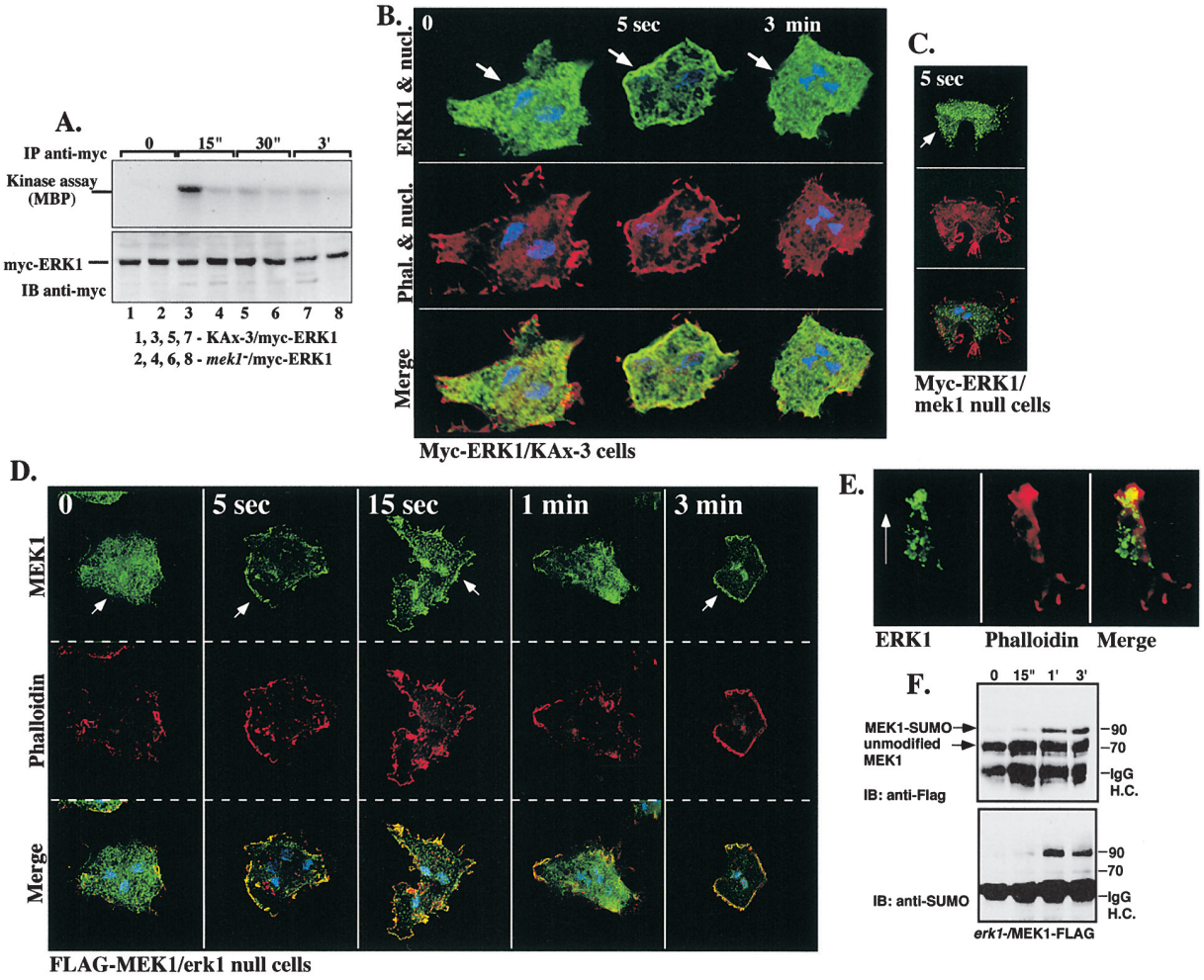

Figure 3. ERK1 Activity and Cortical Localization in Response to cAMP

(A) ERK1 is transiently activated in response to cAMP and MEK1 is required for ERK1 activity. The activity of myc-tagged ERK1 was examined by immune complex kinase assays (upper panel).

(B and C) MEK1-dependent ERK1 localization in response to global cell stimulation with cAMP. Triple labeling of ERK1 with phalloidin and nuclei.

(B) Wild-type cells.

(C) *mek1* null cells.

(D) Involvement of ERK1 in the feedback control of MEK1 localization. FLAG-MEK1 was expressed in *erk1* null cells and its localization and that of F-actin were examined by immunofluorescence using anti-FLAG and TRITC-labeled phalloidin.

(E) Localization of ERK1 and F-actin in chemotaxing cells. The arrow shows the direction of cell movement.

(F) SUMOylation of MEK1 *in erk1* null cells.

To determine whether ERK1 exerts feedback influence on the MEK1 subcellular localization, we expressed MEK1-FLAG in *erk1* null cells and examined the subcellular localization of MEK1 and F-actin in response to cAMP stimulation. Within 5 s, MEK1 translocated to the cell cortex, where it colocalized with F-actin and was still strongly concentrated in the membrane as long as 3 min after cAMP stimulation (Figure 3D). The sustained MEK1 membrane localization in *erk1* null cells was accompanied by an increased and prolonged MEK1 SUMOylation (Figure 3F). Both these results suggest that feedback phosphorylation by ERK1 could be involved in SUMO deconjugation and removal of MEK1 from the plasma membrane.

Chemoattractant-Mediated SUMO Conjugation Is Coupled to MEK1 Activation and Translocation of MEK1 to the Cell Membrane

To examine the possible relationship between the activation of MEK1 and modification by SUMO, we employed the nonactivatable MEK1 (MEK1^{S444A,T448A}; Ma et al., 1997) coexpressed with HA-SUMO. We observed no SUMOylated forms of MEK1^{S444A,T448A} before or after cAMP stimulation (Figure 4A) and there was no observable accumulation of MEK1^{S444A,T448A} at the cell cortex after stimulation (Figure 4C).

To further address the possible role of MEK1 activation in MEK1 SUMOylation, we used constitutively active MEK1 (MEK1^{S444E,T448E}; Ma et al., 1997) and found that it

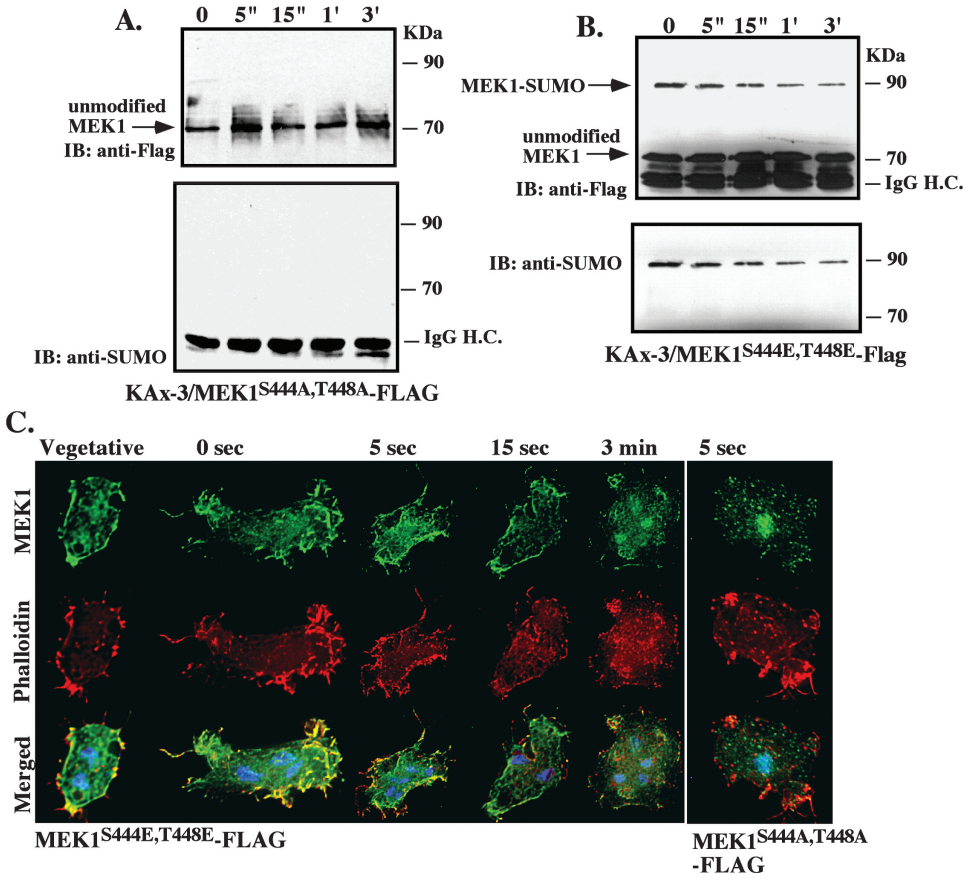

Figure 4. SUMOylation and Localization of MEK1^{S444A,T448A} and MEK1^{S444E,T448E} Mutants

(A) MEK1 activation is coupled to SUMOylation. MEK1^{S444A,T448A} is not modified by SUMO. SUMO conjugation was examined as described in the legend to Figure 1.

(B) MEK1 activation is coupled to SUMOylation. FLAG-MEK1^{S444E,T448E} was expressed in *mek1* null cells and examined for SUMOylation as described above.

(C) Localization of MEK1^{S444A,T448A} and MEK1^{S444E,T448E} mutants. MEK1-phalloidin double labeling was examined as described above.

was constitutively cytosolic, and, in part, present in the cortex of vegetative and unstimulated, aggregation-competent cells (Figure 4C), colocalizing with F-actin. In addition, MEK1^{S444E,T448E} was constitutively SUMOylated, and the level of modification did not increase in response to stimulation, although it decreased slightly at later times (Figure 4B). These results suggest that activation of MEK1 is linked to its SUMOylation.

Regulation of MEK1 Function and Localization through a RING Finger-Containing Interacting Protein

We used a yeast two-hybrid screen with MEK1 as bait to identify potential MEK1-interacting proteins. One of the proteins identified, MIP1 (MEK1-interacting protein 1), has a long N-terminal region with a coiled-coil domain, a polyproline domain, and an acidic domain that lacks sequence homology to known proteins. The MIP1 C-terminal domain encodes a C_3HC_4 RING finger that is highly homologous to respective domains of E3 ubiquitin ligases (Figures 5A and 5B; GenBank accession number AF446007). A putative nuclear localization sequence lies immediately N-terminal to the RING finger domain. Pairwise yeast two-hybrid interaction assays using MIP1 and MEK1 deletion mutants showed that the two proteins interact through their N-terminal domains. In MEK1, the interacting domain is located within residues 58–148 (the deletion endpoints), whereas the interacting region in MIP1 lies between residues 152 and 226 (data not shown). As depicted in Figure 5D, when FLAG-MEK1 was coexpressed with myc-MIP1, both proteins coimmunoprecipitated, indicating that they interact in vivo. The amount of MIP1 that coimmunoprecipitates with MEK1 was lowest in unstimulated cells and increased with time after cAMP stimulation.

We investigated the potential function of MIP1 by analyzing the phenotypes of a *mip1* null strain (see Experimental Procedures) and wild-type cells overexpressing MIP1 or expressing the MIP1 RING finger. *mip1* null cells were less polarized in chemoattractant gradients, moved more slowly and with less directionality than wild-type cells (Figure 1C), and, when plated for multicellular development, produced large aggregates, some of which arrest at the mound stage (Figure 5C). These phenotypes are similar to those of cells expressing constitutively active MEK1^{S444E,T448E} (Ma et al., 1997). In contrast, strains expressing MIP1 or the MIP1 RING finger

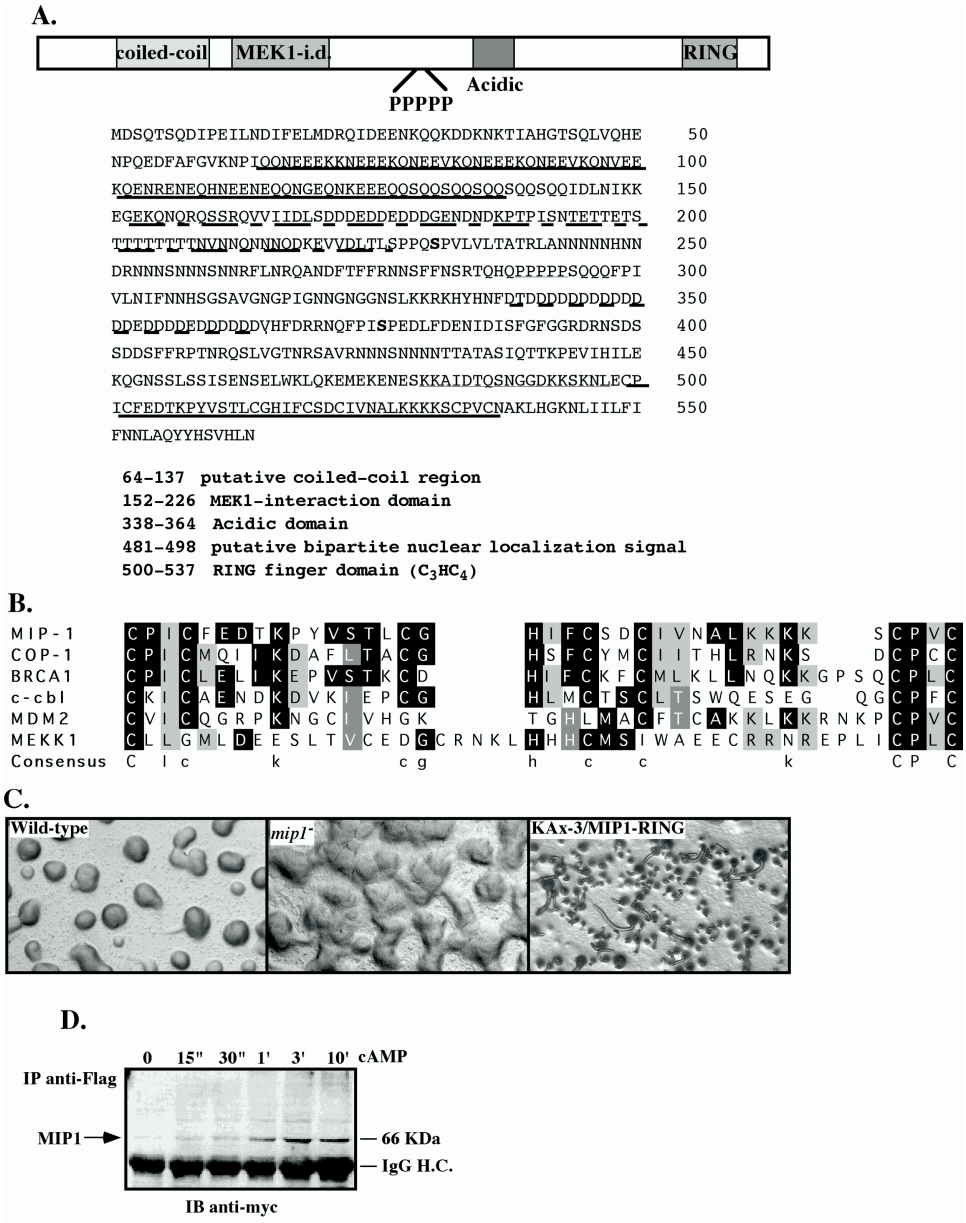

Figure 5. Primary Structure and Functions of MIP1, a MEK1-Associated Protein

(A) The domain composition and primary structure of MIP1, as predicted by SMART, ProSite, and InterProScan sequence analyses. The presence of a putative bipartite nuclear localization signal is consistent with MIP1's nuclear localization. S231 and S376 (bold) are putative MAP kinase phosphorylation sites.

(B) ClustalW sequence alignment demonstrates that the MIP1 C_3HC_4 RING finger shares highest homology with BRCA1, COP1, and SP-RING finger SUMO ligases. Two cysteine residues absent in SP-RING fingers are present in MIP1 and other ubiquitin-specific E3 RING finger proteins.

(C) The morphology of *mip1* null and wild-type KAx-3 cells overexpressing a MIP-RING construct at the aggregation stage of development.

(D) MEK1 and MIP1 associate in vivo as determined by coimmunoprecipitation and Western blot analysis.

domain exhibited chemotaxis and aggregation phenotypes similar to those of *mek1* null cells (Figure 5C). Taken together, these data suggest genetic interactions between MIP1 and MEK1 consistent with MIP1 exhibiting a negative effect on MEK1 function.

To examine functional interactions between MEK1 and MIP1, we studied the subcellular localization of MIP1 and MEK1 before and after chemoattractant stimulation in *mip1* null cells and wild-type cells overexpressing wild-type MIP1 or the MIP1 RING finger. Myc-tagged MIP1 is predominantly nuclear in unstimulated and stimulated cells (Figure 6D). In contrast to our observations in wild-type cells, MEK1 is predominantly cytosolic in *mip1* null cells prior to stimulation, with some

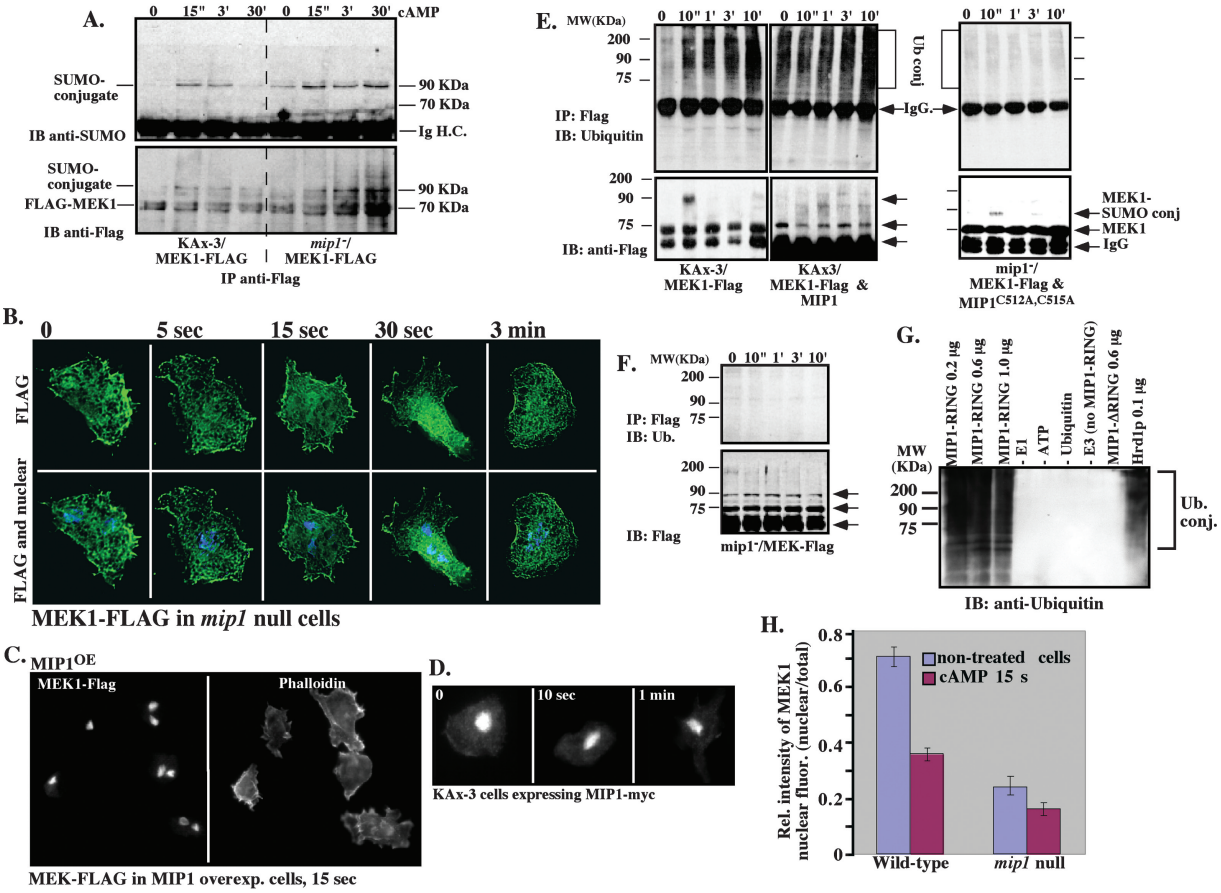

Figure 6. The Effect of MIP1 on MEK1 Ubiquitination, SUMOylation, and Localization

(A) MEK1 SUMOylation was assayed in *mip1* null cells as described in the legend to Figure 1.

(B) Localization of MEK1 in *mip1* null cells.

(C) The effect of MIP1 overexpression on MEK1 localization.

(D) Localization of MIP1 in wild-type cells. An NLS-RING finger C-terminal fragment of MIP1 also localizes to the nucleus (data not shown), suggesting that it contains a nuclear targeting signal.

(E and F) The effect of MIP1 on MEK1 ubiquitination. In vivo MEK1 ubiquitination in response to cAMP stimulation was examined by immunoprecipitation-immunoblot analysis with anti-FLAG and anti-ubiquitin antibodies.

(G) In vitro ubiquitin ligase activity of the MIP1 RING finger. Purified recombinant E1 and E2 were incubated with either MIP1-RING, MIP1-ΔRING, or the known E3 ligase Hrd1p with ATP and ubiquitin at 25°C for 90 min. The control reactions with GST-MIP1-RING and without individual components (-E1, -ATP, and -ubiquitin) are also shown. Anti-ubiquitin immunoblotting was used for detection.

(H) Quantitation and comparison of nuclear MEK1 fluorescence between the wild-type and *mip1* null cells.

of the protein localized to the cell cortex, colocalizing with F-actin (Figures 6B and 6H).

Upon cAMP stimulation, the amount of cortically localized MEK1 in *mip1* null cells increased and appeared to be highest 15 s after stimulation (Figure 6B). In contrast, MEK1 is predominantly nuclear both prior to and after cAMP stimulation in cells overexpressing wild-type MIP1 or a MIP1 deletion that contains only the MIP1 RING finger (MIP1-RING; Figure 6C). Expression of MIP1 containing a disrupted RING finger domain (MIP1^{C512A,C515A}) in *mip1* null cells produced normal and large size aggregates with a partial mound-arrest phenotype, the same phenotype observed for *mip1* null cells (data not shown). In these cells, MEK1 is mostly cytosolic and localizes to the cortex upon cAMP stimulation (data not shown). The reciprocal patterns of MEK1 distribution between the cytosol and nucleus in *mip1* null compared to MIP1-overexpressing cells imply that MIP1 contributes to the nuclear targeting of MEK1. Overexpression studies suggest that an intact, nondisrupted MIP1 RING finger and the whole MIP1 protein may sequester MEK1 in the nucleus.

MIP1 Is Required for MEK1 Ubiquitination but Not SUMOylation

As MIP1 directly associates with the region within the MEK1 N terminus, which contains the SUMO conjugation site, we tested whether MIP1 could play a role in this modification. As shown in Figure 6A, MEK1 is strongly SUMOylated in *mip1* null cells, indicating that MIP1 is not directly required for this modification. Together with the chemotaxis/aggregation defects of the cells, overexpressing MIP1 and SUMOylation-deficient MEK1 mutants, these data argue against the possibility that MIP1 is a MEK1 E3 SUMO ligase. In *mip1* null cells, the level of MEK1 SUMOylation increases after cAMP stimulation

and remains elevated as long as 30 min after cAMP addition, consistent with a model in which targeting MEK1 to the nucleus by MIP1 could counteract and limit SUMOylation and membrane localization of MEK1.

When Western blots of immunoprecipitated FLAG-MEK1 were subjected to the long exposures, in addition to the ~90 kDa SUMOylated MEK1 band, we observed a higher molecular weight "smear" containing MEK1 which was more prominent at later time points (3–30 min) after chemoattractant stimulation (data not shown). The pattern suggested that MEK1 might also be ubiquitinated. When Western blots were probed with an anti-ubiquitin antibody, we observed a smear, indicating these slower mobility isoforms represent polyubiquitinated MEK1 (Figure 6E). In contrast to the very rapid kinetics of MEK1 SUMOylation, the kinetics of MEK1 ubiquitination, as determined by the appearance of polyubiquitinated MEK1, are extended, with the levels being highest at later time points when MEK1 is lost from the plasma membrane and reaccumulates in the nucleus.

As the MIP1 RING finger domain exhibits strongest homology to RING fingers demonstrated to have E3 ubiquitin ligase activity (Figure 5B), we examined whether MIP1 was required for MEK1 ubiquitination. When MEK1 ubiquitination was tested in *mip1* null cells expressing FLAG-MEK1, no ubiquitinated forms of MEK1 were observed (Figure 6F). In contrast, overexpression of MIP1 (Figure 6F) or expression of the MIP1 RING finger domain (data not shown) leads to an increased MEK1 ubiquitination, as compared to the wild-type cells. There was no detectable MEK1 ubiquitination in *mip1* null cells expressing the MIP1 RING finger mutation (MIP1^{C512A,C515A}; Figure 6E, right panel), suggesting that an intact RING finger is required for MEK1 ubiquitination. To test whether MIP1 has a RING finger-dependent E3 ubiquitin ligase activity, GST-fusion proteins corresponding to the C-terminal RING finger domain (MIP1-RING) and the deletion fragment lacking the RING domain and C terminus of MIP1 (MIP1-ΔRING) were assayed in vitro for self-ubiquitination (Bays et al., 2001). Figure 6G reveals strong E1- and ATP-dependent self-ubiquitination of MIP1-RING and the yeast ubiquitin E3 Hrd1p, which was used as a positive control (Figure 6G; Bays et al., 2001). MIP1-ΔRING was found to have no detectable E3 activity. These results directly demonstrate catalytic ubiquitin ligase activity of MIP1-RING domain.

We also examined the ubiquitination of non-SUMOylated (FLAG-tagged MEK1^{K105R}) and nonactivatable (FLAG-tagged MEK1^{S444A,T448A}) forms of MEK1 expressed in *mek1* null cells. Although neither form of MEK1 is SUMOylated, both are ubiquitinated with the kinetics similar to those of the wild-type MEK1 (i.e., it was increased 1–3 min after cAMP stimulation; data not shown). Analysis of cells expressing MEK1^{K105R} suggests that ubiquitin is attached to lysine residues other than K105R, although we can not exclude the possibility that Lys105 may also be a site of ubiquitination. Our results demonstrate that K105R SUMOylation is not required to trigger MEK1 ubiquitination, and MEK1 ubiquitination does not require MEK1 activation (i.e., in *mek1* null cells expressing MEK1^{S444A,T448A}).

Discussion

The MEK1/ERK1 MAP Kinase Cascade Is Spatially and Temporally Regulated

Previous studies demonstrated that *Dictyostelium* MEK1 is required for proper aggregation, morphogenesis, and chemotaxis (Ma et al., 1997). In this manuscript, we have further defined the *mek1* null cell chemotaxis defect, demonstrating quantitatively that these cells exhibit reduced polarity, produce a high frequency of changes in direction, and move slowly compared to wild-type cells under our experimental conditions. Furthermore, we find that the *Dictyostelium* MAP kinase ERK1 lies downstream from MEK1 to control MEK1-mediated pathways. ERK1 is rapidly and transiently activated in response to chemoattractant stimulation and is dependent on MEK1 function. The fact that ERK1 activity is maximal at the 15 s time point and then rapidly decreases suggests that this MAP kinase pathway functions in the initial stages of responses to chemoattractant stimulation. As the chemotaxis phenotypes of the *erk1* and *mek1* null cells are quite severe, with strong defects in cell polarity, directionality, and speed, we suggest that the ERK1/MEK1 MAP kinase cascade controls multiple effector pathways controlling chemotaxis. We found that, like several PH domain-containing proteins (Chung et al., 2001; Parent and Devreotes, 1999; Rickert et al., 2000), both MEK1 and ERK1 transiently localize to the cell cortex in response to chemoattractant stimulation and to the leading edge in chemotaxing cells. Although it is difficult to compare the kinetics of ERK1 activation and ERK1 and MEK1 membrane localization, our results suggest that the responses are highly coordinated, consistent with this MAP kinase pathway playing a key role in chemotaxis. However, we cannot exclude the possibility that the pathway also has a transcriptional role in regulating the developmental state of the cells.

MEK1 SUMOylation Is Required for Its Localization to the Cytosol and Cortex in Response to cAMP

SUMOylation is thought to be involved in the localization of a variety of cellular proteins, although a direct requirement of SUMOylation for subcellular localization has not been proven in some cases. RanGAP1 was one of the first SUMO substrates identified (Matunis et al., 1996). Whereas non-SUMOylated RanGAP1 is cytosolic, SUMOylated RanGAP1 localizes to the cytosolic filaments of the nuclear pore complex, where it interacts with the Ran binding protein 2 (RanBP2) and may play a role in nuclear cytoplasmic protein transport (Melchior, 2000; Kehlenbach et al., 1999; Azuma and Dasso, 2002). SUMO conjugation controls the nuclear import of the *Drosophila* transcription factor Bicoid and the NF-κB homolog Dorsal, and the intranuclear accumulation of the papillomavirus E1 protein (see Muller et al., 2001). In *S. cerevisiae*, the most prominent substrates for SUMO conjugation are the Septins, cytoskeletal GTP binding proteins, which are required for bud growth and cytokinesis, and localize to a ring at the bud neck during mitosis (Johnson and Blobel, 1999).

We demonstrate that MEK1 is modified by SUMOylation in response to chemoattractant stimulation with kinetics that are coincident with MEK1's translocation

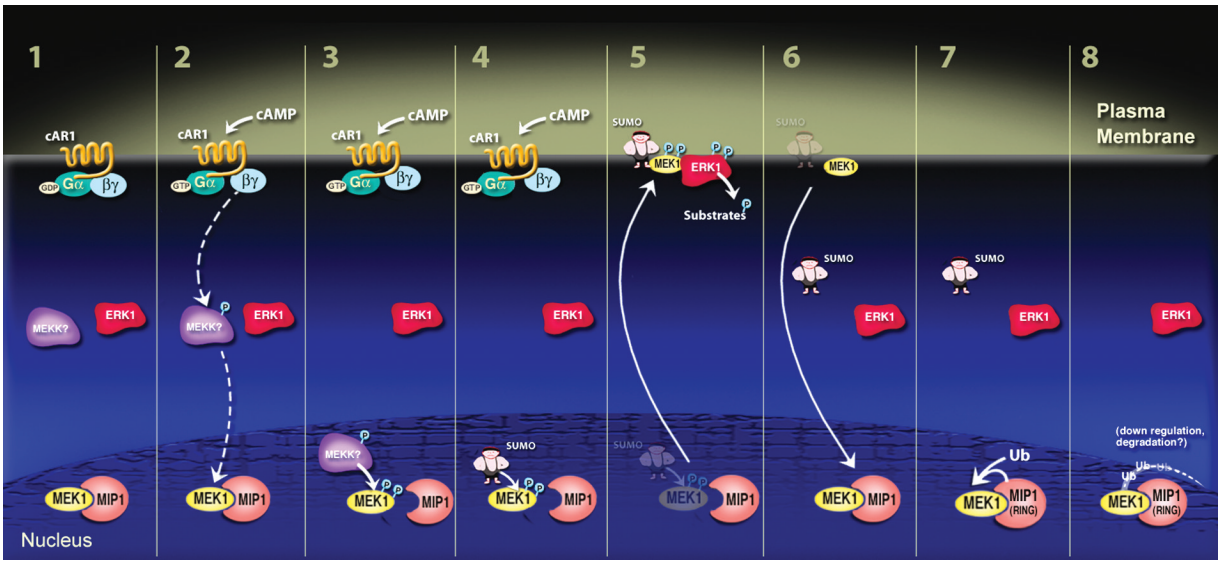

Figure 7. Model for the Role of SUMOylation and MIP1 in the Control of MEK1 Localization in Response to Chemoattractant Stimulation

The cartoon shows the activation of distinct components of the MAP kinase pathway and their dynamic relocalization in response to cAMP, depicted as consecutive steps 1–8 (see text). MEK1 is concentrated in the nucleus prior to stimulation. cAMP stimulation is coupled to the activation of putative MEKK, which in turn activates MEK1. Activated MEK1 is rapidly SUMOylated and exported out of the nucleus, being targeted to the cell cortex. ERK1 is activated and recruited to the cell cortex, where we suggest it phosphorylates the set of substrate proteins. MEK1 is rapidly dephosphorylated and de-SUMOylated and then becomes resequestered in the nucleus, where it associates with MIP1 and is ubiquitinated. The dual function of MIP1 is nuclear sequestration of MEK1 and E3 ubiquitin ligase activity mediating MEK1 ubiquitination, both leading to the termination of the signal. Possible alternative models are presented in the Discussion.

from the nucleus to the cytosol and cortex within the limits of resolution of our studies. Our mutational analysis indicates that Lys105 is the site of SUMOylation. Our results show that MEK1^{K105R} predominantly remains in the nucleus after chemoattractant stimulation. These data suggest that SUMOylation is required for exit from the nucleus and/or localization to the cell's cortex with SUMOylation functioning as part of a nuclear export and/or cortical localization signal. The connection between SUMOylation and nucleocytoplasmic transport is further supported by the demonstration that RanBP2, a regulator of nuclear protein import and export (Kehlenbach et al., 1999), exhibits E3 SUMO ligase activity (Pichler et al., 2002; Azuma and Dasso, 2002). We cannot exclude an alternate model in which MEK1 is in a dynamic nucleocytoplasmic equilibrium that is slanted in the direction of nuclear localization in unstimulated cells and shifted to a cytosolic/cortical localization with SUMOylation, possibly inhibiting MEK1 transport into the nucleus. Although we cannot formally exclude this model, we do not favor it because of the localization properties of other MEK1 and MIP1 mutant proteins.

We further demonstrate that MEK1^{S444A,T448A}, which cannot be activated, is not SUMOylated and remains nuclear, whereas constitutively active MEK1^{S444E,T448E} is found predominantly in the cytosol and on the plasma membrane, even in vegetative and aggregation-competent unstimulated cells. As a significant fraction (but not all) of MEK1^{S444E,T448E} is constitutively SUMOylated, we suggest that activation of MEK1 is the signal that leads to its SUMOylation. In *mip1* null cells, the major portion of MEK1 is cytosolic in unstimulated cells with a portion being SUMOylated. The level of SUMO-MEK1 increases significantly after cAMP stimulation. We note that not all of the MEK1 becomes SUMOylated or localizes to the cortex in response to signaling. It is possible that this is due to the expected higher-than-wild-type levels of MEK1 and MIP1 that are expressed in our stably transformed strains. This results from the high copy number of the tandemly repeated integrated vector (Nellen and Firtel, 1985). Higher-than-wild-type level MEK1 in these strains may saturate the SUMOylation or upstream activation machinery, possibly resulting in a limited fraction of the MEK1 being activated and/or SUMOylated. It is also possible that MEK1 may have nuclear functions and only a portion of MEK1 is SUMOylated and localizes to the cortex.

Our data suggest the regulatory pathway presented in Figure 7. Although other scenarios are possible, we propose that nuclearly localized MEK1 is activated, possibly in the nucleus, by a yet-to-be identified upstream kinase leading to its SUMOylation, coupled to transport to the cytosol, and localization to the cell cortex in response to global stimulation and to the leading edge in chemotaxing cells. ERK1 is recruited and activated by MEK1 and also localizes to the cell's cortex. As some MEK1 is cytoplasmic in unstimulated cells, we cannot exclude the possibility that part of the MEK1 that localizes to the cortex comes from this cytoplasmic pool. Although the mechanism of MEK1 inactivation is unknown, the observation that constitutively active MEK1^{S444E,T448E} is cytosolic and constitutively SUMOylated while inactive MEK1^{S444A,T448A} is nuclear suggests that the first step in MEK1 adaptation may be a dephosphorylation of the MEK1 activation loop, followed by deSUMOylation, which leads to the loss of cortical localization and re-

transport to the nucleus. As MEK1 is SUMOylated for an extended time in *erk1* null cells, it is possible that a feedback phosphorylation by ERK1 leads to de-SUMOylation. The kinetics of MEK1 ubiquitination suggest that the process is activated or increases in rate in response to cAMP stimulation. Our cartoon depicts this occurring in the nucleus, as MIP1 is predominantly nuclear, and MIP1 is required for MEK1 ubiquitination. MEK1^{S444E,T448E} is also ubiquitinated (our unpublished observations), which may occur in the nucleus, as not all MEK1^{S444E,T448E} is cytosolic.

MIP1 Is a Putative Ubiquitin E3 Ligase that Controls MEK1 Localization and Ubiquitination

Our combined genetic and biochemical evidence suggests that MIP1 is a MEK1 ubiquitin E3 ligase. The recombinant RING finger of MIP1, which is highly homologous to known RING finger E3 ligases, shows strong ubiquitin ligase activity in vitro; *mip1* null cells do not exhibit MEK1 ubiquitination, whereas MEK1 is hyperubiquitinated in cells overexpressing MIP1 or the MIP1 RING finger domain; MIP1 and MEK1 directly associate in a yeast two-hybrid assay and interact in vivo as determined by coimmunoprecipitation. The in vivo association is strongest several minutes after chemoattractant stimulation, coincident with the kinetics of ubiquitination. However, we cannot exclude the possibility that the effect of MIP1 on MEK1 is indirect, and MIP1 could function as E3 ligase for an unknown protein in the same complex.

We show that overexpression of MIP1 leads to the retention of MEK1 in the nucleus after chemoattractant stimulation and constitutive ubiquitination. In agreement with the observed aggregation defect, it is possible that overexpression of MIP1 is sufficient to prevent MEK1's activation, SUMOylation, and transport to the cytosol. We observe a much lower level of MEK1 protein in MIP1-overexpressing cells than in wild-type cells. In contrast, in *mip1* null cells and cells expressing MIP1^{C512A,C515A}, the steady-state levels of MEK1 protein are significantly higher, even though the levels of MEK1 transcripts in all these strains are the same (data not shown). This finding suggests that MEK1 protein may exhibit a rapid rate of turnover in MIP1-overexpressing cells, possibly through an increased level of ubiquitination and degradation.

Mammalian MEKK1 has an E3 ubiquitin ligase RING finger domain, suggesting that MEKK1 mediates the degradation of a subset of cellular proteins. We previously demonstrated that the *Dictyostelium* MEKK, MEKKα, which has an F box and WD40 repeats as part of the protein and is important in controlling cell fate decisions in *Dictyostelium*, is regulated through preferential degradation in a cell type-specific manner (Chung et al., 1998). Furthermore, the presence of the RING domain in yeast Ste5 suggests that one or more components of the pheromone-activated MAP kinase cascade may be ubiquitinated. It is possible that one method of downregulating some MAP kinase signaling pathways is through ubiquitination.

In this manuscript, we have provided the evidence that a MAP kinase pathway that is essential for proper development and chemotaxis in *Dictyostelium* is regulated by differential SUMOylation and ubiquitination. As MAP kinase pathways are also required for the cell migration of fibroblasts (Giroux et al., 1999; Yujiri et al., 2000), there may be a commonality of function of MAP kinase pathways in this evolutionarily conserved cellular response. Interestingly, mammalian MEK1 and MEK2 and MEKs in yeast, plants, and fungi have sequences in their N termini fitting the I/LKXE(D) consensus for SUMO conjugation (see Supplemental Table S1 at http://www.developmentalcell.com/cgi/content/full/3/1/■■■/DC1), but it is unknown whether these proteins are SUMOylated in response to signaling and whether this may regulate their function. It is intriguing that one of these motifs in MEK1 and MEK2 is the part of well-characterized, leucine-rich MEK nuclear export signal (NES). Nishida and coworkers (Fukuda et al., 1996, 1997) found that disruption of this motif by mutagenesis prevents the CRM1-mediated translocation of MEK1 out of the nucleus. The absence of an obvious NES in *Dictyostelium* MEK1 may explain why it is concentrated in the nuclei of nonstimulated cells and why it is not constitutively excluded from the nuclei, as occurs with mammalian MEK1. MEK1 SUMOylation could represent an ancient conserved mechanism controlling subcellular localization of these proteins.

Experimental Procedures

Molecular Biology

MIP1 (GenBank accession number AF446007) was identified in a yeast two-hybrid screen, using the full-length MEK1 as bait. To knock out MIP1, a BamHI linker was inserted at the PvuII site of the MIP1 sequence and a fragment containing a blasticidin-resistant Bsr gene cassette. The complete DdSUMO gene sequence (GenBank accession number AF446008) was identified by using the *Dictyostelium* genome BLAST search. ORFs encoding MIP1 and DdSUMO were amplified by PCR using a *Dictyostelium* cDNA library and subcloned into *Dictyostelium* expression vectors (Ma et al., 1997). Mutants were obtained using the Transformer kit (Clontech) or the QuickChange mutagenesis kit. FLAG-, myc-, and HA-tagged sequences were added in-frame by PCR. The sequence of amplified DNA was confirmed by sequencing.

Materials

Protein A and G Sepharose were obtained from Sigma and Santa Cruz Biotechnology. TRITC-phalloidin, myelin basic protein (MBP), protein kinase inhibitors, and protease inhibitors were from Sigma. Recombinant human E1, E2 (Ubc4), ubiquitin, and Hrd1p were generous gifts from R. Hampton (UCSD).

Anti-FLAG monoclonal antibody (M2) was from Sigma. Antibodies to the myc tag were obtained from Invitrogen and Santa Cruz. Anti-HA (12CA5) antibodies were from Roche and Santa Cruz. Anti-human SUMO1 antibodies were from Zymed and Santa Cruz. Goat anti-mouse and anti-rabbit FITC- and TRITC-conjugated antibodies were from Sigma and Jackson ImmunoResearch. Anti-mouse and anti-rabbit HRP-conjugated antibodies were from Amersham Biosciences.

Cell Biology and Biochemistry

The *Dictyostelium* strains used and methods employed have been previously described (Ma et al., 1997). Chemotaxis assays and image acquisition were carried out as described previously (Chung and Firtel, 1999). Cell movement and cell shape were analyzed using DIAS software (Solltech; Wessels and Soll, 1998).

To measure ERK1 kinase activity, cells were assayed as described for Akt kinase activity (Meili et al., 1999), except that myc-ERK1 was immunoprecipitated using anti-myc antibody, with MBP as the substrate. SDS-PAGE and immunoblotting were carried out using standard procedures with the ECL kit (Amersham) for detection.

Recombinant GST MIP1-RING and MIP1-ΔRING fusion proteins were purified using glutathione agarose and used in an in vitro self-ubiquitination assay with human recombinant E1 and E2 (Ubc4), as described (Bays et al., 2001).

For immunofluorescence microscopy, images were acquired with a DeltaVision deconvolution microscope system in the UCSD Cancer Center Digital Imaging Core. Data sets were deconvolved and analyzed using SoftWorx software (Applied Precision; Agard et al., 1989) on a Silicon Graphics Octane workstation.

MEK1 fluorescence intensities of deconvolved images were acquired in equal rectangular boxes at three positions (nucleus, cytosol, and cell membrane) along radial axes connecting the areas of measurement and analyzed using SoftWorx. Relative intensities of fluorescence in the cell membrane and nuclei shown on the graphs with respective standard deviations represent average values of 20 to 25 measurements and are determined as ($I_{MEMBRANE}$ / [$I_{MEMBRANE}$ + $I_{CYTOSOL}$ + $I_{NUCLEUS}$]) and ($I_{NUCLEUS}$ / [$I_{MEMBRANE}$ + $I_{CYTOSOL}$ + $I_{NUCLEUS}$]), respectively. The paired two-sample t test was used for the statistical analysis of quantitative data.

Acknowledgments

We would like to thank J. Feramisco and S. McMullen, UCSD Cancer Center Digital Imaging Shared Resource, for helpful suggestions and expert technical assistance. We thank N. Iranfar and W. Loomis for the initial ERK1 REMI mutant. We thank O. Bazirgan, N. Bays, and R. Hampton for assistance in the ubiquitination assays and R. Hampton and members of the Firtel laboratory for helpful suggestions. A.S. was funded in part by a Long Term EMBO Postdoctoral Fellowship (ALTF-47, 1999). The work was supported by USPHS grants to R.A.F.

Received: December 18, 2001
Revised: April 10, 2002

References

Agard, D.A., Hiraoka, Y., Shaw, P.J., and Sedat, J.W. (1989). Fluorescence microscopy in three dimensions. Methods Cell Biol. *30*, 353–377.

Azuma, Y., and Dasso, M.A. (2002). New clue at the nuclear pore: RanBP2 is an E3 enzyme for SUMO1. Dev. Cell *2*, 130–132.

Bays, N.W., Gardner, R.G., Seelig, L.P., Joazeiro, C.A., and Hampton, R.Y. (2001). Hrd1p/Der3p is a membrane-anchored ubiquitin ligase required for ER-associated degradation. Nat. Cell Biol. *3*, 24–29.

Bernier-Villamor, V., Sampson, D.A., Matunis, M.J., and Lima, C.D. (2002). Structural basis for E2-mediated SUMO conjugation revealed by a complex between ubiquitin-conjugating enzyme Ubc9 and RanGAP1. Cell *108*, 345–356.

Buschmann, T., Fuchs, S., Lee, C., Pan, Z., and Ronai, Z. (2000). SUMO-1 modification of Mdm2 prevents its self-ubiquitination and increases Mdm2 ability to ubiquitinate p53. Cell *101*, 753–762.

Chung, C., and Firtel, R. (1999). PAKa, a putative PAK family member, is required for cytokinesis and the regulation of the cytoskeleton in *Dictyostelium discoideum* cells during chemotaxis. J. Cell Biol. *147*, 559–576.

Chung, C., Reddy, T., Zhou, K., and Firtel, R. (1998). A novel, putative MEK kinase controls developmental timing and spatial patterning in *Dictyostelium* and is regulated by ubiquitin-mediated protein degradation. Genes Dev. *12*, 3564–3578.

Chung, C., Funamoto, S., and Firtel, R. (2001). Signaling pathways controlling cell polarity and chemotaxis. Trends Biochem. Sci. *26*, 557–566.

Desterro, J., Rodriguez, M., and Hay, R. (1998). SUMO-1 modification of IκBα inhibits NF-κB activation. Mol. Cell *2*, 233–239.

Fukuda, M., Gotoh, I., Gotoh, Y., and Nishida, E. (1996). Cytoplasmic localization of mitogen-activated protein kinase kinase directed by its NH2-terminal, leucine-rich short amino acid sequence, which acts as a nuclear export signal. J. Biol. Chem. *271*, 20024–20028.

Fukuda, M., Asano, S., Nakamura, T., Adachi, M., Yoshida, M., Yanagida, M., and Nishida, E. (1997). CRM1 is responsible for intracellular transport mediated by the nuclear export signal. Nature *390*, 308–311.

Gaskins, C., Maeda, M., and Firtel, R. (1994). Identification and functional analysis of a developmentally regulated extracellular signal-regulated kinase gene in *Dictyostelium discoideum*. Mol. Cell. Biol. *10*, 6996–7012.

Giroux, S., Tremblay, M., Bernard, D., Cardin-Girard, J., Aubry, S., Larouche, L., Rousseau, S., Huot, J., Landry, J., Jeannotte, L., and Charron, J. (1999). Embryonic death of Mek1-deficient mice reveals a role for this kinase in angiogenesis in the labyrinthine region of the placenta. Curr. Biol. *9*, 369–372.

Hochstrasser, M. (2001). Sp-Ring for SUMO. New functions bloom for a ubiquitin-like protein. Cell *106*, 735–744.

Johnson, E., and Blobel, G. (1999). Cell cycle-regulated attachment of the ubiquitin-related protein SUMO to the yeast septins. J. Cell Biol. *147*, 981–994.

Kehlenbach, R.H., Dickmanns, A., Kehlenbach, A., Guan, T., and Gerace, L. (1999). A role for RanBP1 in the release of CRM1 from the nuclear pore complex in a terminal step of nuclear export. J. Cell Biol. *145*, 645–657.

Ma, H., Gamper, M., Parent, C., and Firtel, R. (1997). The *Dictyostelium* MAP kinase kinase DdMEK1 regulates chemotaxis and is essential for chemoattractant-mediated activation of guanylyl cyclase. EMBO J. *16*, 4317–4332.

Matunis, M., Coutavas, E., and Blobel, G. (1996). A novel ubiquitin-like modification modulates the partitioning of the Ran-GTPase-activating protein RanGAP1 between the cytosol and the nuclear pore complex. J. Cell Biol. *135*, 1457–1470.

Meili, R., Ellsworth, C., Lee, S., Reddy, T.B.K., Ma, H., and Firtel, R.A. (1999). Chemoattractant-mediated transient activation and membrane localization of Akt/PKB is required for efficient chemotaxis to cAMP in *Dictyostelium*. EMBO J. *18*, 2092–2105.

Melchior, F. (2000). SUMO—nonclassical ubiquitin. Annu. Rev. Cell Dev. Biol. *16*, 591–626.

Muller, S., Hoege, C., Pyrowolakis, G., and Jentsch, S. (2001). SUMO, ubiquitin's mysterious cousin. Nat. Rev. Mol. Cell Biol. *2*, 202–210.

Nellen, W., and Firtel, R.A. (1985). High-copy-number transformants and co-transformation in *Dictyostelium*. Gene *39*, 155–163.

Parent, C.A., and Devreotes, P.N. (1999). A cell's sense of direction. Science *284*, 765–770.

Pichler, A., Gast, A., Seeler, J.S., Dejean, A., and Melchior, F. (2002). The nucleoporin RanBP2 has SUMO1 E3 ligase activity. Cell *108*, 109–120.

Rickert, P., Weiner, O., Wang, F., Bourne, H., and Servant, G. (2000). Leukocytes navigate by compass: roles of PI3K-γ and its lipid products. Trends Cell Biol. *10*, 466–473.

Sampson, D., Wang, M., and Matunis, M. (2001). The small ubiquitin-like modifier-1 (SUMO-1) consensus sequence mediates Ubc9 binding and is essential for SUMO-1 modification. J. Biol. Chem. *276*, 21664–21669.

Soll, D.R., and Wessels, D. (1998). Motion Analysis of Living Cells (New York: Wiley-Liss).

Wessels, D., and Soll, D.R. (1998). Computer-assisted characterization of the behavioral defects of cytoskeletal mutants of *Dictyostelium discoideum*. In Motion Analysis of Living Cells, D.R. Soll and D. Wessels, eds. (New York: Wiley-Liss), pp. 101–140.

Yujiri, T., Ware, M., Widmann, C., Oyer, R., Russell, D., Chan, E., Zaitsu, Y., Clarke, P., Tyler, K., Oka, Y., et al. (2000). MEK kinase 1 gene disruption alters cell migration and c-Jun NH2-terminal kinase regulation but does not cause a measurable defect in NF-κ B activation. Proc. Natl. Acad. Sci. USA *97*, 7272–7277.

Accession Numbers

The GenBank accession numbers for the MIP1 and complete DdSUMO sequences are AF446007 and AF446008, respectively.